AFRL-VA-WP-TP-2006-318

APPLICATION OF PIECEWISE LINEAR CONTROL ALLOCATION TO REUSABLE LAUNCH VEHICLE GUIDANCE AND CONTROL (PREPRINT)

Michael A. Bolender
David B. Doman
Michael W. Oppenheimer

FEBRUARY 2006

Approved for public release; distribution is unlimited.

STINFO COPY

AIR VEHICLES DIRECTORATE
AIR FORCE MATERIEL COMMAND
AIR FORCE RESEARCH LABORATORY
WRIGHT-PATTERSON AIR FORCE BASE, OH 45433-7542

NOTICE

This report was cleared for public release by the Air Force Research Laboratory Wright Site (AFRL/WS) Public Affairs Office (PAO) and is releasable to the National Technical Information Service (NTIS). It will be available to the general public, including foreign nationals.

PAO Case Number: AFRL/WS 06-0577, 28 Feb 2006.

THIS TECHNICAL REPORT IS APPROVED FOR PUBLICATION.

//Signature//

Michael A. Bolender
Aerospace Engineer
Control Design and Analysis Branch
Air Force Research Laboratory
Air Vehicles Directorate

//Signature//

Brian W. Van Vliet
Chief
Control Sciences Division
Air Force Research Laboratory
Air Vehicles Directorate

REPORT DOCUMENTATION PAGE

Form Approved
OMB No. 0704-0188

1. REPORT DATE *(DD-MM-YY)*	2. REPORT TYPE	3. DATES COVERED *(From - To)*
February 2006	Conference Paper Preprint	05/01/2002– 01/31/2006

4. TITLE AND SUBTITLE
APPLICATION OF PIECEWISE LINEAR CONTROL ALLOCATION TO REUSABLE LAUNCH VEHICLE GUIDANCE AND CONTROL (PREPRINT)

5a. CONTRACT NUMBER
In-house

5b. GRANT NUMBER

5c. PROGRAM ELEMENT NUMBER
N/A

6. AUTHOR(S)
Michael A. Bolender
David B. Doman
Michael W. Oppenheimer

5d. PROJECT NUMBER
A03D

5e. TASK NUMBER
N/A

5f. WORK UNIT NUMBER
0B

7. PERFORMING ORGANIZATION NAME(S) AND ADDRESS(ES)
Control Design and Analysis Branch (AFRL/VACA)
Control Sciences Division
Air Vehicles Directorate
Air Force Materiel Command, Air Force Research Laboratory
Wright-Patterson Air Force Base, OH 45433-7542

8. PERFORMING ORGANIZATION REPORT NUMBER
AFRL-VA-WP-TP-2006-318

9. SPONSORING/MONITORING AGENCY NAME(S) AND ADDRESS(ES)
Air Vehicles Directorate
Air Force Research Laboratory
Air Force Materiel Command
Wright-Patterson Air Force Base, OH 45433-7542

10. SPONSORING/MONITORING AGENCY ACRONYM(S)
AFRL/VACA

11. SPONSORING/MONITORING AGENCY REPORT NUMBER(S)
AFRL-VA-WP-TP-2006-318

12. DISTRIBUTION/AVAILABILITY STATEMENT
Approved for public release; distribution is unlimited.

13. SUPPLEMENTARY NOTES
This work has been submitted to the Mediterranean Control Association for publication in the 2006 14th Mediterranean Conference on Control and Automation Proceedings. This is a work of the U.S. Government and is not subject to copyright protection in the United States.

PAO Case Number: AFRL/WS 06-0577 (cleared February 28, 2006). Report contains color.

14. ABSTRACT

We will demonstrate two applications of the piecewise linear control allocation (PLCA) approach. The first application to be considered is to use the PLCA approach in the inner-loop control law of a re-usable launch vehicle on approach and landing. Body axis angular rates are controlled using a dynamic inversion controller. The vehicle will be subjected to two stuck control effectors, and recovery of the vehicle using only control effector reconfiguration provided by the control allocator and without trajectory reshaping will be demonstrated. The second application that will be demonstrated is constraint estimation for trajectory reshaping and re-targeting. In order to successfully re-target a trajectory when an aircraft has experienced degraded performance due to a failure or damage to the vehicle, the effects of the failure or damage on the lift, drag, and "trimmability" of the vehicle must be known a priori over the entire flight envelope. We present a method that allows for the effects of a locked or floating control effector to be estimated over the flight envelope.

15. SUBJECT TERMS
Control Allocation, Redundant Actuators, Trajectory Optimization, Control Theory

16. SECURITY CLASSIFICATION OF:			17. LIMITATION OF ABSTRACT:	18. NUMBER OF PAGES	19a. NAME OF RESPONSIBLE PERSON (Monitor)
a. REPORT	b. ABSTRACT	c. THIS PAGE			Michael A. Bolender
Unclassified	Unclassified	Unclassified	SAR	16	19b. TELEPHONE NUMBER *(Include Area Code)* N/A

Standard Form 298 (Rev. 8-98)
Prescribed by ANSI Std. Z39-18

Application of Piecewise Linear Control Allocation to Reusable Launch Vehicle Guidance and Control

(Invited Paper)

Michael A. Bolender
Control Design and Analysis Branch
Air Force Research Laboratory
Wright-Patterson AFB, OH 45433
Michael.Bolender@wpafb.af.mil

David B. Doman
Control Design and Analysis Branch
Air Force Research Laboratory
Wright-Patterson AFB, OH 45433
David.Doman@wpafb.af.mil

Michael W. Oppenheimer
Control Design and Analysis Branch
Air Force Research Laboratory
Wright-Patterson AFB, OH 45433
Michael.Oppenheimer@wpafb.af.mil

***Abstract*— The moments produced by the aerodynamic control effectors on aircraft are typically non-linear functions of displacement with a region of linearity about zero displacement. For nominal operation with no locked or floating effectors and for gentle maneuvers, affine approximations to the moment displacement curves are sufficient as the effectors operate primarily in the linear region. However, if an actuator has become locked and/or aggressive maneuvering is required, the control effectors may require large deflections into the non-linear regions of the moment-displacement curve in order to maximize the available control power. As we move away from the linear region, the affine approximation becomes inaccurate, especially in cases where the slope of the moment curve changes sign. In this paper we will briefly review a novel approach that was developed at AFRL for solving the control allocation problem where the control moments are piecewise linear functions of the control displacement. The advantages of this approach are that it avoids cumbersome, high-order polynomial curve fits of the aerodynamic data and thus avoids solution of a non-linear programming problem. Stability and control derivatives are almost always stored in multi-dimensional look-up tables where it is assumed that the data is piecewise linear. The approach that is presented utilizes this piecewise linear assumption for the control effector moment data and accounts for non-linearities in the moment-effector relationships and position constraints on the effectors as well. The control allocation problem using piecewise linear functions is posed as a mixed-integer linear program (MILP) and solved using a freely available GNU-licensed mixed-integer linear programming code.**

We will demonstrate two applications of the piecewise linear control allocation (PLCA) approach. The first application to be considered is to use the PLCA approach in the inner-loop control law of a re-usable launch vehicle on approach and landing. Body axis angular rates are controlled using a dynamic inversion controller. The vehicle will be subjected to two stuck control effectors, and recovery of the vehicle using only control effector reconfiguration provided by the control allocator and *without* trajectory reshaping will be demonstrated. However, the downside of the MILP formulation is that the optimization problem cannot be solved fast enough for real-time implementation on the current generation of flight control computers.

The second application that will be demonstrated is constraint estimation for trajectory reshaping and re-targeting. In order to successfully re-target a trajectory when an aircraft has experienced degraded performance due to a failure or damage to the vehicle, the effects of the failure or damage on the lift, drag, and "trimmability" of the vehicle must be known *a priori* over the entire flight envelope. We present a method that allows for the effects of a locked or floating control effector to be estimated over the flight envelope. This method has the advantage of including six degree-of-freedom effects (i.e., trimmability) in the point-mass models used by trajectory synthesis algorithms. For situations where there are stuck or floating control effectors, the aerodynamic data does not change; therefore, the effects of the failure can be estimated over the entire flight envelope. We will show how to determine constraints on the trajectory using the PLCA approach that was outlined above. However, the "preference vector" used in the control allocator requires careful consideration along with the specific type of trajectory desired (e.g., computation of the maximum downrange vs. minimum downrange for the footprint), otherwise adverse interactions between the control allocator and the trajectory synthesizer may occur.

I. Principles of Control Allocation

Our interest in control allocation is motivated by the development of re-configurable control laws for autonomous aerospace vehicles. One such class of vehicles is the next generation of re-usable launch vehicles. The next generation of RLVs will be characterized by a minimal control effector suite to facilitate control re-configuration when the aircraft experiences either failures in the flight control system or damage to the vehicle. Typically, at the inner-most control loop, the control system is controlling body-axis angular rates to meet the outer-loop guidance commands. When the number of effectors exceeds the number of controlled variables, it is quite common that the desired commands can be achieved in many different ways. A control allocation algorithm can be used to find a set of control effector positions that meet some desired objective in addition to delivering the desired angular rates. Additionally, the control effectors are subject to position and/or rate limiting constraints that can be enforced by a well designed control allocation algorithm.

Control allocation can be stated simply as follows: Given the mapping

$$\boldsymbol{d}_{des} = \boldsymbol{G}(\boldsymbol{\delta}) \tag{1}$$

subject to:

$$\boldsymbol{\delta} \in [\boldsymbol{\delta}_{min}, \boldsymbol{\delta}_{max}] \tag{2}$$

$$\dot{\boldsymbol{\delta}} \in [\dot{\boldsymbol{\delta}}_{min}, \dot{\boldsymbol{\delta}}_{max}] \tag{3}$$

where $\boldsymbol{d}_{des} \in \mathbb{R}^m$ and $\boldsymbol{\delta} \in \mathbb{R}^n$ and $n > m$, we desire to find the inverse mapping such that

$$\boldsymbol{\delta} = \boldsymbol{G}^{-1}(\boldsymbol{d}_{des}) \tag{4}$$

such that the constraints $\boldsymbol{\delta} \in [\boldsymbol{\delta}_{min}, \boldsymbol{\delta}_{max}]$ and $\dot{\boldsymbol{\delta}} \in [\dot{\boldsymbol{\delta}}_{min}, \dot{\boldsymbol{\delta}}_{max}]$ are not violated.

To solve the control allocation problem, it is usually assumed that the control moments produced by the control effectors are linear functions of the effector displacement

$$\boldsymbol{G}(\boldsymbol{\delta}) = \boldsymbol{B}\boldsymbol{\delta} \tag{5}$$

This has led to much research being devoted to various methods for solving what we will call the *linear control allocation problem*. The linear control allocation problem is often re-stated as an equivalent optimization problem (either a linear or quadratic program) in order to ensure that the limits on the control effector positions and rates are satisfied (see References [1], [2], [3]). Non-optimization approaches do exist, primarily those attributed to Durham [4].

The assumption that the moments are linear functions of the effectors is quite valid for most control effectors about their primary control axis, thus linear control allocation approaches are successful under nominal flight conditions. In this case small non-linearities are seen as disturbances or model uncertainty and the control laws are robust enough that system stability and performance are not compromised. However, there are situations where the effectors must operate away from the linear region, or when it may be beneficial to take advantage of the non-linear effects. In these cases, we want to include the effects of the non-linearities in the control allocation. One situation is when the aircraft has a stuck effector, and the moment producing capability about a secondary axis is highly non-linear. For example, for left-right pairs of effectors, there is a quadratic relationship between the yawing moment and the effector displacement. In this case, deflection of a single effector on one side of the vehicle induces a yawing moment to that side of the vehicle due to the asymmetric drag distribution. This yawing moment occurs for both positive and negative deflections of the control surface. In this case a linear fit can only be applied to one side of the curve, otherwise we have a gross mismodelling of the moment-effector relationship.

One approach that was designed to account for benign non-linearities, and has been successfully flight-tested, was developed at AFRL by Oppenheimer and Doman [5]. Their approach added an "intercept-correction" term that made the relationship between the controls and the moments affine: $\boldsymbol{B}\boldsymbol{\delta} + \boldsymbol{\varepsilon} = \boldsymbol{d}_{des}$. However, this approach is still limiting because there may be slope reversals in the aerodynamic data. The possibility exists where the allocator could become captured in this non-linear region, resulting in actuator saturation.

To further improve control allocation and to maximize the performance of the effector suite on the aircraft requires taking advantage of the non-linearities present in the data. Non-linear programming approaches were not of interest due to the fact that polynomials on the order of 5 or higher were typically needed to accurately fit the aerodynamic data, thus resulting in a rather difficult set of equations to solve. A more natural approach is to utilize the inherent piecewise linear nature of the aerodynamic data. This is the approach that we pursued in Reference [6], and is outlined here for completeness.

II. Piecewise Linear Programming

Piecewise linear programming is an optimization method that allows one to approximate non-linear programming problems that are comprised of separable functions. To solve the resulting approximation problem, a linear program can be formulated and then solved using a modified simplex method [7]. A second option is to formulate the non-linear program as a mixed-integer linear program [8].

In terms of control allocation, the restriction of approximating separable functions by piecewise linear functions may appear to be overly restrictive. For most aircraft, the control induced moments can be considered as separable since, in many cases, there are no significant aerodynamic interactions among the control effectors. In some instances the cross-coupling of control effectors cannot be neglected, such as when control effectors are located downstream of other surfaces or when two effectors are located adjacent to one another.

For purposes of illustration, we will approximate a single-valued function, $f(x)$, by its piecewise linear approximation and show how to formulate the minimization of $f(x),\ x \in [a, b]$ as a piecewise linear program. The approach given below for a single variable function can be generalized for multi-variable, separable functions rather easily. Furthermore, we are not restricted to only approximating the objective function by a piecewise linear approximation since it is also possible to consider piecewise linear approximations of the constraints, if they are separable, within the same framework. A detailed discussion can be found in Reklaitis, et.al. [7].

Without loss of generality, we begin by considering a single variable function, $f(x)$, defined on an interval, $[a, b]$. Begin by defining a grid of K points spaced on the interval $[a, b]$ and denote these points as $x^{(k)}$, $k = 1, \ldots, K$ where $a = x^{(1)} < x^{(2)} < \cdots < x^{(k)} < \cdots < x^{(K)} = b$. Note that we are not restricted to a uniform spacing of the $x^{(k)}$. Furthermore, let $f^{(k)}$ denote the value of $f(x^{(k)})$. A piecewise linear approximation of $f(x)$ can then be constructed by connecting $(x^{(k)}, f^{(k)})$ and $(x^{(k+1)}, f^{(k+1)})$ with a straight line as shown in Figure 1. The equation of the line connecting the points $(x^{(k)}, f^{(k)})$ and $(x^{(k+1)}, f^{(k+1)})$ is given by

$$\tilde{f}(x) = f^{(k)} + \frac{f^{(k+1)} - f^{(k)}}{x^{(k+1)} - x^{(k)}}(x - x^{(k)}) \tag{6}$$

where $x \in [x^{(k)}, x^{(k+1)}]$. There will be $K - 1$ such equations, one for each subinterval. Observe that on a given subinterval, x can be written as

$$x = \lambda^{(k)} x^{(k)} + \lambda^{(k+1)} x^{(k+1)} \tag{7}$$

where $\lambda^{(k)} \geq 0$ and $\lambda^{(k+1)} \geq 0$. The $\lambda^{(k)}$ are normalized such that

$$\lambda^{(k)} + \lambda^{(k+1)} = 1 \tag{8}$$

It can then be shown that Equation 6 can be written as

$$\tilde{f}(x) = \lambda^{(k)} f^{(k)} + \lambda^{(k+1)} f^{(k+1)}$$

Therefore, in the interval $[x^{(1)}, x^{(K)}]$, a given value of the approximate value $\tilde{f}(x)$ can be determined by ass appropriate values to $\lambda^{(k)}$ and $\lambda^{(k+1)}$ that correspond subinterval in which x lies. Since x can only be define single subinterval, all the $\lambda^{(k)}$ which are not associate that particular interval all must be equal to zero. As a we can express Equations 7 and 9 as

$$x = \sum_{k=1}^{K} \lambda^{(k)} x^{(k)}$$
$$\tilde{f}(x) = \sum_{k=1}^{K} \lambda^{(k)} f^{(k)}$$

subject to the following conditions:

$$\sum_{k=1}^{K} \lambda^{(k)} = 1 \tag{12}$$
$$\lambda^{(k)} \geq 0,\ k = 1, \ldots, K \tag{13}$$

and

$$\lambda^{(i)} \lambda^{(j)} = 0 \quad \text{if } j > i+1;\ i = 1, \ldots, K-1 \tag{14}$$

Equation 14 is necessary to ensure that only points lying on piecewise linear segments that connect adjacent breakpoints are considered as part of the approximating function. For example, given a value of x, no more than two of the $\lambda^{(k)}$'s are allowed to be non-zero and positive, and the two $\lambda^{(k)}$'s also must be adjacent. If we consider a value of x where $\lambda^{(3)}$ and $\lambda^{(4)}$ are positive, with $\lambda^{(1)} = \lambda^{(2)} = 0$ and $\lambda^{(k)} = 0, k = 5, \ldots, K$, then the value of $\tilde{f}(x)$ lies on the approximating function between $x^{(3)}$ and $x^{(4)}$. On the other hand, if $\lambda^{(4)} > 0$ was to be replaced by $\lambda^{(6)} > 0$, and all other $\lambda^{(k)} = 0$, then the line connecting $x^{(3)}$ and $x^{(6)}$ would not be part of the approximating function. Furthermore, if we chose a value of x such that $x = x^{(k)}$ and $\tilde{f}(x) = f(x)$, then from Equation 12, $\lambda^{(k)} = 1$ and all other values of $\lambda = 0$. Lastly, it is important to note that one can always obtain a more accurate approximation of $f(x)$ by increasing the number of gridpoints; however, this obviously increases the size of problem.

Given that we now have a piecewise linear approximation to $f(x)$ and the additional constraints that result from the transformation, we are able to state the Piecewise Linear Program that corresponds to the minimization of $f(x)$ on the interval $a \leq x \leq b$.

$$\min \tilde{f}(x) = \sum_{k=1}^{K} \lambda^{(k)} f^{(k)} \tag{15}$$

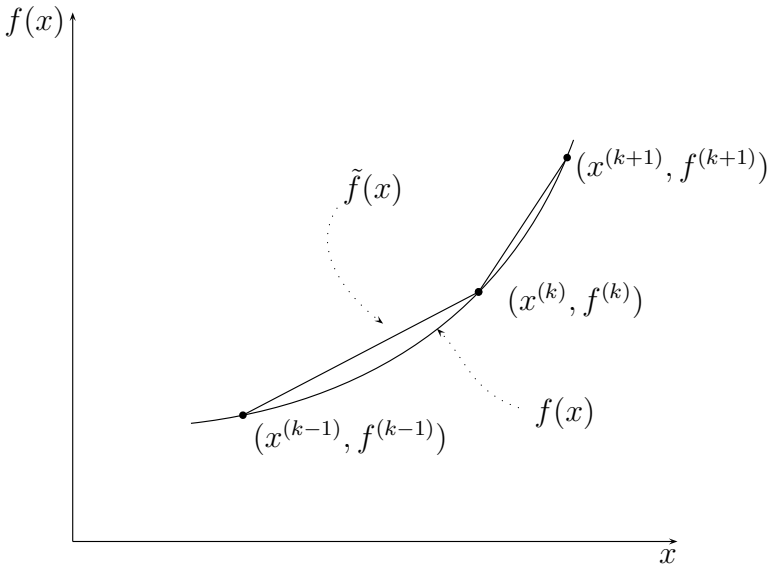

Fig. 1. Piecewise Linear Function Approximation

subject to

$$\sum_{k=1}^{K} \lambda^{(k)} = 1 \tag{16}$$
$$\lambda^{(k)} \geq 0 \tag{17}$$

Once the solution to the piecewise linear program is obtained, one uses Equation 10 to find the corresponding value of x that gives an approximate minimum to $f(x)$. Finding a solution to a piecewise linear program requires an approach that ensures that Equation 14 is satisfied. Recall that Equation 14 requires that no more than two adjacent $\lambda^{(k)}$'s are allowed to be non-zero. Therefore, to find an optimal feasible solution to the piecewise linear program, one of two approaches must be taken. One approach is to solve the problem using the simplex method with a restricted basis entry rule. [7] A second approach is to formulate Equation 14 using binary decision variables [8] that will constrain x to be on only one subinterval. The result will be yet another increase in the size of the problem beyond what was necessary for the piecewise linear approximation. The addition of the binary variables transforms the piecewise linear programming problem into a mixed-integer linear program (MILP). We will take the latter approach because it is sufficient for demonstrating the validity of the approach, and also because of the availability of an open-source code (GNU Linear Programming Kit) that solves linear programs and mixed-integer linear programs.

A. Transformation of the Piecewise Linear Program to a Mixed-Integer Linear Program

Begin by considering the piecewise linear approximation shown in Figure 1. Note that if there are K breakpoints, then

there are $K-1$ linear segments. We assign a variable $y^{(k)}$ that corresponds to the k^{th} linear segment of the piecewise linear approximation such that

$$y^{(k)} = \begin{cases} 1 & \text{if } \lambda^{(k)} \neq 0 \text{ and } \lambda^{(k+1)} \neq 0, \\ 0 & \text{otherwise} \end{cases} \tag{18}$$

for $k = 1, \ldots, K-1$. Next, we make the observation that if $\lambda^{(1)} \neq 0$ and $\lambda^{(2)} \neq 0$, then

$$\lambda^{(1)} \leq y^{(1)} \tag{19}$$
$$\lambda^{(2)} \leq y^{(1)} \tag{20}$$

where $y^{(1)} = 1$. However, if we are on the segment where $\lambda^{(2)} \neq 0$ and $\lambda^{(3)} \neq 0$, such that $y^{(2)} = 1$, then

$$\lambda^{(2)} \leq y^{(2)} \tag{21}$$
$$\lambda^{(3)} \leq y^{(2)}. \tag{22}$$

If we proceed in this manner, we observe that the following restrictions can be placed on the $\lambda^{(k)}$

$$\lambda^{(1)} \leq y^{(1)}, \tag{23}$$
$$\lambda^{(k)} \leq y^{(k-1)} + y^{(k)}, \; k = 2, \ldots, K-1 \tag{24}$$
$$\lambda^{(K)} \leq y^{(K-1)}. \tag{25}$$

The rationale behind Equation 24 is as follows: the $\lambda^{(k)}$ that correspond to points that are interior to the interval (i.e., they are not the endpoints of the interval on which x is defined) can be associated with one of two line segments. A particular $\lambda^{(k)}$ is an endpoint for the line segment immediately preceding it in addition to the line segment that comes immediately after it. Only one of these two line segments may be "active" at any time; therefore, the right-hand side of Equation 24 is never greater than one. In addition to Equations 23-25, we have an additional constraint to ensure that only one of the $K-1$ line segments is active, hence only one of the $y^{(k)}$ can be equal to one:

$$\sum_{k=1}^{K-1} y^{(k)} = 1 \tag{26}$$

By including Equations 23-26 into the piecewise linear program for the arbitrary single valued function being minimized in the example above, we transform it into a mixed integer linear program. The transformed optimization problem is stated as follows:

$$\min \tilde{f}(x) = \sum_{k=1}^{K} \lambda^{(k)} f^{(k)} \tag{27}$$

subject to

$$\sum_{k=1}^{K} \lambda^{(k)} = 1 \tag{28}$$
$$\lambda^{(k)} \geq 0 \tag{29}$$
$$\lambda^{(1)} \leq y^{(1)} \tag{30}$$
$$\lambda^{(k)} \leq y^{(k-1)} + y^{(k)}, \; k = 2, \ldots, K-1 \tag{31}$$
$$\lambda^{(K)} \leq y^{(K-1)} \tag{32}$$
$$\sum_{k=1}^{K-1} y^{(k)} = 1 \tag{33}$$
$$y^{(k)} \in \{0, 1\} \tag{34}$$

By including the additional constraints which are necessary to complete the transformation of the piecewise linear program, we have added an additional $K-1$ decision variables to the problem. This does not include any slack or surplus variables that may be required by the solver to convert inequality constraints into equality constraints. The slack and surplus variables will further increase the number of decision variables. The solution to the mixed integer linear program is obtained by using a branch-and-bound algorithm. Technical details on the branch-and-bound algorithm can be found in Bertsimas [8].

III. Piecewise Linear Mixed Optimization Control Allocation

The control allocation problem solved in Reference [6] used two distinct performance indices that were similar to those used in Buffington's [2] multi-branch approach. However, instead of a linear relationship between the control effector displacements and the control moments, a non-linear relationship was used. Let the non-linear vector-valued function $\boldsymbol{G}(\boldsymbol{\delta})$ denote the relationship between the control effector positions and their moments. The function $\boldsymbol{G}(\boldsymbol{\delta})$ maps $\mathbb{R}^n$ into $\mathbb{R}^m$ where $n \geq m$ and n is the number of control effectors and m is the number of controlled variables. Let $\boldsymbol{d}_{des}$ denote the controlled variables. In this case the controlled variables are the rolling, pitching and yawing moments. Buffington's multi-branch approach requires that two optimization problems be solved. The first optimization problem is called the control deficiency branch. The objective of the control deficiency branch is to minimize $\|\boldsymbol{W}_a(\boldsymbol{G}(\boldsymbol{\delta}) - \boldsymbol{d}_{des})\|_1$ subject to position and rate constraints on $\boldsymbol{\delta}$. The value of the performance index for this optimization problem indicates whether or not $\boldsymbol{d}_{des}$ is feasible. If feasibility of the control allocation problem has been ascertained, a second optimization problem is then solved that minimizes some secondary objective. The objective function of this second optimization is typically taken to be $\|\boldsymbol{W}_u(\boldsymbol{\delta} - \boldsymbol{\delta}_p)\|_1$ subject to $\boldsymbol{G}(\boldsymbol{\delta}) = \boldsymbol{d}_{des}$ and position and rate constraints on $\boldsymbol{\delta}$. This is commonly referred to as the control sufficiency branch.

The mixed optimization problem that was formulated by Bodson [3] combines the two branches of the multi-branch control allocation problem into a single optimization problem.

A new parameter ϵ is introduced for the purpose of prioritizing either control deficiency or control sufficiency. The mixed optimization problem is stated as:

$$\min J = ||\boldsymbol{W}_a(\boldsymbol{G}(\boldsymbol{\delta}) - \boldsymbol{d}_{des})||_1 + \epsilon||\boldsymbol{W}_u(\boldsymbol{\delta} - \boldsymbol{\delta}_p)||_1 \quad (35)$$

subject to:

$$\boldsymbol{\delta}_{min} \leq \boldsymbol{\delta} \leq \boldsymbol{\delta}_{max} \quad (36)$$

where $\boldsymbol{W}_a = \text{diag}(w_{a1}, w_{a2}, w_{a3}, \ldots, w_{am})$ is a weighting matrix used to prioritize a given control axis, $\boldsymbol{G}(\boldsymbol{\delta})$ is a non-linear, vector-valued function that maps $\mathbb{R}^n$ to $\mathbb{R}^m$, $\boldsymbol{\delta}$ is an $n \times 1$ vector of control effectors, $\boldsymbol{W}_u = \text{diag}(w_{u1}, w_{u2}, w_{u3}, \ldots, w_{un})$ is a weighting matrix on the control effectors, and $\boldsymbol{\delta}_p$ is an $n \times 1$ vector of "preferred" control effector displacements. Again it is assumed that $n \geq m$. For the moment we will make the assumption that $\boldsymbol{G}(\boldsymbol{\delta}) = \boldsymbol{B\delta}$. The mixed optimization problem can then be posed as a linear programming problem. The corresponding linear program can then be solved by any readily-available linear programming software.

Bodson [3] gives one possible transformation to a linear programming problem for the optimization problem defined in Equations 35 and 36; however, we selected a transformation approach that can be found in Bertsimas [8]. The transformation relies on the observation that $|x|$ is the smallest number x_s that satisfies both $x \leq x_s$ and $-x \leq x_s$. As a result, we are able to pose the mixed optimization problem as follows:

$$\min J = \boldsymbol{W}_a\boldsymbol{\delta}_s + \epsilon\boldsymbol{W}_u\boldsymbol{u}_s \quad (37)$$

subject to:

$$\boldsymbol{\delta}_s \geq 0 \quad (38)$$
$$\boldsymbol{u}_s \geq 0 \quad (39)$$
$$\boldsymbol{B\delta} + \boldsymbol{\delta}_s \geq \boldsymbol{d}_{des} \quad (40)$$
$$-\boldsymbol{B\delta} + \boldsymbol{\delta}_s \geq -\boldsymbol{d}_{des} \quad (41)$$
$$\boldsymbol{\delta} + \boldsymbol{u}_s \geq \boldsymbol{\delta}_p \quad (42)$$
$$-\boldsymbol{\delta} + \boldsymbol{u}_s \geq -\boldsymbol{\delta}_p \quad (43)$$
$$\boldsymbol{\delta}_{min} \leq \boldsymbol{\delta} \leq \boldsymbol{\delta}_{max} \quad (44)$$

The vectors $\boldsymbol{\delta}_s$ and $\boldsymbol{u}_s$ are vectors of "slack variables". The reason for selecting this particular transformation as opposed to the one in Bodson [3] is that this formulation allows us to easily implement the piecewise linear function approximation.

To convert the linear programming problem into a piecewise linear programming problem, we simply replace $\boldsymbol{B\delta}$ above with a piecewise linear representation of each control moment curve, (i.e., $\bar{L}_i(\delta_i)$, $M_i(\delta_i)$, and $N_i(\delta_i)$). We choose a set of breakpoints for each $\delta_i,\ i = 1, \ldots, n$ such that:

$$\delta_i = \sum_{k=1}^{K_i} \lambda_i^{(k)} \delta_i^{(k)} \quad (45)$$

$$\sum_{k=1}^{K_i} \lambda_i^{(k)} = 1 \quad (46)$$

$$\lambda_i^{(j)}\lambda_i^{(k)} = 0, \quad \text{if } k > j+1,\ j = 1, \ldots, K_i - 1 \quad (47)$$

where $\lambda_i^{(k)}$ is a non-negative interpolating coefficient corresponding to the i^{th} control effector at breakpoint k, and K_i denotes the number of breakpoints for the i^{th} control effector. Equation 47 is necessary in order ensure that δ_i is approximated by no more than two *adjacent* values of $\lambda_i^{(k)}$. If δ_i falls at a breakpoint, there will only be one value of $\lambda_i^{(k)}$ that is non-zero and Equation 47 is still valid.

For inner-loop flight control, we assume that our objective is to find a set of control deflections $\boldsymbol{\delta}$ such that a specified rolling moment L, pitching moment, M, and yawing moment N are simultaneously achieved. The piecewise linear approximations for the control moments as a function of δ_i are written as

$$\bar{L}_i = \bar{L}(\delta_i) = \sum_{k=1}^{K_i} \lambda_i^{(k)} \bar{L}_i^{(k)} \quad (48)$$

$$M_i = M(\delta_i) = \sum_{k=1}^{K_i} \lambda_i^{(k)} M_i^{(k)} \quad (49)$$

$$N_i = N(\delta_i) = \sum_{k=1}^{K_i} \lambda_i^{(k)} N_i^{(k)} \quad (50)$$

where $\bar{L}_i^{(k)}$, $M_i^{(k)}$, and $N_i^{(k)}$ are the values of the rolling, pitching, and yawing moment curves evaluated at the k^{th} breakpoint for the i^{th} control effector. We are now able to replace $\boldsymbol{B\delta}$ with $\tilde{\boldsymbol{B}}\boldsymbol{\Lambda}$ where

$$\tilde{\boldsymbol{B}} = \begin{bmatrix} \bar{L}_1^{(1)} & \bar{L}_1^{(2)} & \ldots & \bar{L}_i^{(k)} & \ldots & \bar{L}_n^{(K_n)} \\ M_1^{(1)} & M_1^{(2)} & \ldots & M_i^{(k)} & \ldots & M_n^{(K_n)} \\ N_1^{(1)} & N_1^{(2)} & \ldots & N_i^{(k)} & \ldots & N_n^{(K_n)} \end{bmatrix} \quad (51)$$

and

$$\boldsymbol{\Lambda} = \begin{bmatrix} \lambda_1^{(1)} \\ \lambda_1^{(2)} \\ \vdots \\ \lambda_i^{(k)} \\ \vdots \\ \lambda_n^{(K_n)} \end{bmatrix} \quad (52)$$

The vector $\boldsymbol{\Lambda}$ is of length $\sum_{i=1}^{n} K_i$ and $\tilde{\boldsymbol{B}}$ is a matrix of size $n_c \times \sum_{i=1}^{n} K_i$ where n_c is the number of controlled variables. In the piecewise linear optimization problem, the constraints $\boldsymbol{\delta}_{min} \leq \boldsymbol{\delta} \leq \boldsymbol{\delta}_{max}$ are replaced by $\lambda_i^{(k)} \geq 0$. The upper and lower bounds on $\boldsymbol{\delta}$ are accounted for in the selection of the breakpoints for each δ_i. Once we obtain an optimal solution to the problem, we compute each δ_i using Equation 45. It is

also necessary to include in the problem the n constraints that correspond to Equation 46.

The resulting optimization problem is

$$\min J = \boldsymbol{W}_a \boldsymbol{\delta}_s + \epsilon \boldsymbol{W}_u \boldsymbol{u}_s \tag{53}$$

subject to:

$$\boldsymbol{\delta}_s \geq 0 \tag{54}$$

$$\boldsymbol{u}_s \geq 0 \tag{55}$$

$$\tilde{\boldsymbol{B}}\boldsymbol{\Lambda} + \boldsymbol{\delta}_s \geq \boldsymbol{d}_{des} \tag{56}$$

$$-\tilde{\boldsymbol{B}}\boldsymbol{\Lambda} + \boldsymbol{\delta}_s \geq -\boldsymbol{d}_{des} \tag{57}$$

$$\sum_{k=1}^{K_i} \lambda_i^{(k)} \delta_i^{(k)} + u_{s,i} \geq \delta_{p,i}, \quad i = 1, \ldots, n \tag{58}$$

$$-\sum_{k=1}^{K_i} \lambda_i^{(k)} \delta_i^{(k)} + u_{s,i} \geq -\delta_{p,i}, \quad i = 1, \ldots, n \tag{59}$$

$$\lambda_i^{(k)} \geq 0, \quad i = 1, \ldots, n, \quad k = 1, \ldots, K_i \tag{60}$$

$$\sum_{k=1}^{K_i} \lambda_i^{(k)} = 1, \quad i = 1, \ldots, n \tag{61}$$

$$\lambda_i^{(j)} \lambda_i^{(k)} = 0, \quad \text{if } k > j+1,\ j = 1, \ldots, K_i - 1 \tag{62}$$

The constraint given by Equation 62 is enforced using binary variables and a set of explicit constraints on the segments of each piecewise linear control moment as described above. The resulting optimization problem is then a mixed-integer linear program. The additional constraints are

$$\lambda_i^{(1)} \leq y_i^{(1)}, \quad i = 1, \ldots, m \tag{63}$$

$$\lambda_i^{(k)} \leq y_i^{(k-1)} + y_i^{(k)}, \quad i = 1, \ldots, m, \quad k = 2, \ldots, K_i - 1 \tag{64}$$

$$\lambda_i^{K_i} \leq y_i^{(K_i - 1)}, \quad i = 1, \ldots, m \tag{65}$$

$$\sum_{k=1}^{K_i - 1} y_i^{(K_i - 1)} = 1, \quad i = 1, \ldots, m \tag{66}$$

$$y_i^{(k)} \in \{0, 1\} \tag{67}$$

IV. Applications

There are two important applications for control allocation algorithms that take into account the non-linear relationship between the control effectors and the control moments. Our original motivation for the use of non-linear control allocation was adaptive/reconfigurable control systems as a means to maximize the performance by optimally selecting the control deflections to meet the commanded body-axis rotational rates. As will be discussed below, the benefits of non-linear control allocation occur when there are effector failures that require the remaining control effectors to operate in their non-linear regions. In this section, we will compare the performance of the piecewise linear control allocation approach to a linear allocation method in a simulation of a re-entry vehicle that uses a dynamic inversion control law for inner-loop control. A second application of non-linear control allocation is the determination of constraints for use with trajectory reshaping algorithms [9]. Here it is necessary to be able to accurately determine the range of angles-of-attack over which the vehicle can be trimmed in the presence of control effector failures. An additional benefit of solving the constraint estimation problem is that trim lift and drag effects can be included in the trajectory reshaping problem with little additional computational burden. The trim maps and the lift and drag perturbations can re determined off-line and stored on-board in the guidance computer to facilitate real-time trajectory re-shaping.

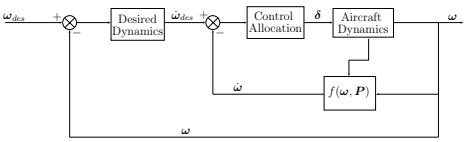

Fig. 2. Block Diagram of Inner-loop Dynamic Inversion Control Law

A. Dynamic Inversion Flight Control

Dynamic inversion controllers attempt to cancel and replace the dynamics of the plant being controlled with a set of desired dynamics. If the fidelity of the on-board reference model is high enough, then the dynamic inversion control law results in a closed-loop system that behaves like a decoupled bank of integrators. In the context of flight control, a common objective of a dynamic inversion control law is to provide good body-axis angular rate tracking.

It is assumed that a pilot or an outer-loop guidance system generates body-axis angular velocity commands P_c, Q_c, R_c. The inner-loop dynamic inversion control law is designed such that the aircraft tracks these angular velocity commands (see Figure 2). The rotational dynamics for an aircraft can be written as:

$$\boldsymbol{I}\dot{\boldsymbol{\omega}} = \boldsymbol{G}_B - \boldsymbol{\omega} \times \boldsymbol{I}\boldsymbol{\omega} \tag{68}$$

where $\boldsymbol{\omega} = \begin{bmatrix} P & Q & R \end{bmatrix}^T$, $\boldsymbol{I}$ is the moment-of-inertia tensor, and $\boldsymbol{G}_B$ are the moments acting on the vehicle. We can express $\boldsymbol{G}_B$ as a sum that includes moments that are due to the wing-body aerodynamics and propulsion system, which we will collectively refer to as the base moments, and moments due to the control effectors:

$$\boldsymbol{G}_B = \boldsymbol{G}_{base}(\boldsymbol{\omega}, \boldsymbol{P}) + \boldsymbol{G}(\boldsymbol{P}, \boldsymbol{\delta}) = \begin{bmatrix} \bar{L} \\ M \\ N \end{bmatrix}_{base} + \begin{bmatrix} \bar{L}(\boldsymbol{\delta}) \\ M(\boldsymbol{\delta}) \\ N(\boldsymbol{\delta}) \end{bmatrix} \tag{69}$$

where $\boldsymbol{G}_{base}(\boldsymbol{\omega}, \boldsymbol{P})$ is the moment generated by the base engine-aerodynamic system and $\boldsymbol{G}(\boldsymbol{P}, \boldsymbol{\delta})$ is the sum of the moments produced by the control effectors. The parameter vector $\boldsymbol{P}$ denotes measurable or estimable quantities that influence the body angular accelerations and includes variables such as Mach number, angle of attack, sideslip angle and vehicle mass properties such as moments of inertia. Thus we define

$$\boldsymbol{f}(\boldsymbol{\omega}, \boldsymbol{P}) \triangleq \boldsymbol{G}_{base}(\boldsymbol{\omega}, \boldsymbol{P}) - \boldsymbol{\omega} \times \boldsymbol{I}\boldsymbol{\omega} \tag{70}$$

The model used for the design of the dynamic inversion control law then becomes:

$$\boldsymbol{I}\dot{\boldsymbol{\omega}} = \boldsymbol{f}(\boldsymbol{\omega}, \boldsymbol{P}) + \boldsymbol{G}(\boldsymbol{P}, \boldsymbol{\delta}) \tag{71}$$

and our objective is to find a control law that provides direct control over $\dot{\boldsymbol{\omega}}$ such that $\dot{\boldsymbol{\omega}} = \dot{\boldsymbol{\omega}}_{des}$, i.e.,

$$\boldsymbol{I}\dot{\boldsymbol{\omega}}_{des} = \boldsymbol{f}(\boldsymbol{\omega}, P) + \boldsymbol{G}(\boldsymbol{P}, \boldsymbol{\delta}) \tag{72}$$

therefore, the inverse control must satisfy:

$$\boldsymbol{I}\dot{\boldsymbol{\omega}}_{des} - \boldsymbol{f}(\boldsymbol{\omega}, \boldsymbol{P}) = \boldsymbol{G}(\boldsymbol{P}, \boldsymbol{\delta}) \tag{73}$$

Since there are more control effectors than controlled variables, a control allocation algorithm must be used to obtain a solution. Solution of this control allocation problem will be discussed in detail in a later section. Equation 73 states that the control effectors are to be used to correct for the difference between the desired accelerations and the accelerations due only to the base moments.

B. Simulation of Dynamic Inversion Control Law

The mixed-integer linear programs for the mixed-optimization control allocation discussed above were implemented in a Simulink simulation of a re-entry vehicle. This particular vehicle has six control surfaces: left and right rudders, left and right flaperons, a body flap, and a speed brake. The simulation models the descent, final approach, and touchdown of the vehicle.

The performance of the piecewise linear approach is compared to that of a linear control allocation method. The linear control allocator assumes that the moments are linear functions of the effectors. The slope of the control moment curve is calculated with respect to the current control effector position using a forward difference approximation. An intercept correction [5] term is then applied to account for mild non-linearities in the aerodynamic data.

The results that follow give the closed-loop vehicle performance when there are two failures injected into the flight control system at different times during the approach and landing phases. It is assumed that there is some type of fault detection capability on-board the aircraft to identify the failures. The failure information is immediately passed to the control allocation algorithm in order to facilitate reconfiguration of the vehicle's effectors. The aircraft's trajectory begins at an altitude of about 15,000 ft above the runway and 4 miles downrange from the runway threshold. The first failure occurs 30 s into the simulation, and involves the body flap being locked at -5 deg. This failure contributes a constant pitching moment to the aircraft. A second failure, where the right rudder becomes locked at 1 deg, occurs at 40 s. This particular failure adds not only a pitching moment to the aircraft, but also rolling and yawing moments. This particular failure combination was chosen because it requires the flaperons to operate in a highly non-linear region of the control moment curve. After the failures are introduced, the aircraft tries to follow the nominal approach trajectory to the runway threshold. The aircraft extends the landing gear at about 68 s and flares immediately before touchdown. The simulation ends at touchdown when the weight-on-wheels switch is triggered.

For the control sufficiency branch of the control allocator, a "preferred" control position, $\boldsymbol{\delta}_p$, is required. There are several different objectives that may be used to determine $\boldsymbol{\delta}_p$. These include, but are not limited to, minimum control deflection ($\boldsymbol{\delta}_p = \mathbf{0}$), minimum 2-norm of deflection, and null-space injection [2], [10]. The preference vector used in this simulation is the minimum 2-norm of the control surface deflection. This particular $\boldsymbol{\delta}_p$ minimizes $\boldsymbol{\delta}^T\boldsymbol{W}\boldsymbol{\delta}$ subject to $\boldsymbol{B}\boldsymbol{\delta} = \boldsymbol{d}_{des}$ where $\boldsymbol{W}$ is a positive definite weighting matrix. For our results, we take the weighting matrix, $\boldsymbol{W}$, as the identity matrix. The corresponding solution to this problem is then $\boldsymbol{\delta}_p = \boldsymbol{B}^T(\boldsymbol{B}\boldsymbol{B}^T)^{-1}\boldsymbol{d}_{des}$. Note that this particular preference vector has the advantage of facilitating robustness analysis with the control allocator in the loop since the control allocator can be represented in closed-form for local linear analysis . For the piecewise linear control allocation, we found that it was sufficient to compute the right pseudo-inverse solution, $\boldsymbol{\delta}_p$, with a $\boldsymbol{B}$ matrix that uses local slopes of the control moments at the last control surface position.

We will measure the performance of the two control allocators by their ability to produce deflections, that when applied to the non-linear aerodynamic database, produce the desired moments about each axis. This metric is an indication of the error that results from the selection of a particular model in the control allocation algorithm.

1) Simulation Results: The results for the piecewise linear control allocator as compared to a linear control allocator with intercept correction are given in Figures 3 and 4. Figure 3 shows the base 10 logarithm of $\|\boldsymbol{d}_{des} - \boldsymbol{G}(\boldsymbol{P}, \boldsymbol{\delta})\|_2$, where $\boldsymbol{G}(\boldsymbol{P}, \boldsymbol{\delta})$ is the moment that is applied to the vehicle when given the control deflections returned by the control allocator. It is evident that the piecewise linear control allocator returns control surface deflections that produce the desired moments. On the other hand, the linear control allocator has a significant error. Note that at the 40s mark, when the second failure is introduced, both control allocators indicate that there is a moment deficiency due to control effector saturation. Beyond 60s the performance of the piecewise linear control allocator improves once the effectors are no longer saturated. The poor performance of the linear control allocator is primarily due to the modelling errors inherent in the linear approximation of the control moment curves. The control surface commands from each control allocator are shown in Figure 4. We see that after the second failure is injected into the simulation that the flaperon deflections saturate at their upper limit. Note that the flap and speedbrake commands for the piecewise linear allocator oscillate after about 65 sec. This appears to be due to an oscillatory $\boldsymbol{d}_{des}$ and $\boldsymbol{\delta}_p$ that result from body-axis rate loop closures. For the linear control allocator, we see that the flaps, left rudder, and speedbrake exhibit large amplitude oscillations. Note that for this failure case, the vehicle that flew with the piecewise linear control allocator maintained controlled flight.

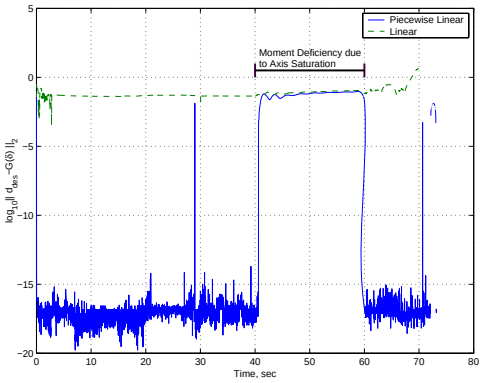

Fig. 3. Difference Between Desired and Applied Moments

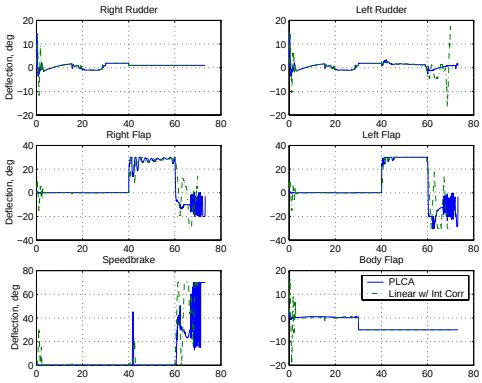

Fig. 4. Control Effector Time History

It should be noted that both the linear and non-linear control allocation approaches were solved using the GNU Linear Programming Kit's linear programming simplex library for the former and the branch-and-bound solver for the latter. The simulation with the non-linear control allocator and the branch-and-bound solver ran extremely slow when compared to the simulation with the linear program solver used for the linear control allocator. It was observed that it took approximately 8.5 times longer on average to find a solution to the MILP control allocation problem as compared to the linear programming approach. This computational burden may limit one's ability to utilize the MILP approach in a real-time, digital flight control system in the near future. Performance gains may be achieved by solving the piecewise linear control allocation problem via the simplex method with the restricted basis entry rules [7].

C. Application to Trajectory Re-shaping

The intent here is to show a second important application of non-linear control allocation. One of the areas of active research regarding reusable launch vehicles is the on-line determination of new feasible trajectories following a control effector failure. It is desired to safely guide the aircraft from the time that the failure occurs to a safe abort and to recover the vehicle if possible. An important part of the determination of feasible trajectories is having accurate estimates of the ranges of angle-of-attack, for a given Mach number, at which the aircraft can be trimmed. Also, it is important to be able to estimate critical parameters, such as the maximum lift-to-drag ratio, that will impact the optimal trajectory [9]. It is not desirable to use a linear control allocation approach to determine whether or not the vehicle can be trimmed. The reason is that a linear control allocator would require a single line of best fit to approximate the moment-deflection curve at a fixed flight condition, thereby introducing significant modelling errors. These modelling errors would then result in an inaccurate determination of the range of trimmable angles-of-attack. On the other hand, using a non-linear control allocation algorithm allows one to more accurately estimate the range of angles-of-attack over which one may trim the aircraft as well as the critical parameters that affect the trajectory, such as trim lift and trim drag.

To solve for the range of angles-of-attack over which the vehicle can be trimmed, we want to determine where in the flight envelope there exists enough available control power to null the wing-body rolling, pitching, and yawing moments. The procedure for this is outlined below in Algorithm 1. If we consider Equation 73, and set $\boldsymbol{\omega} = \dot{\boldsymbol{\omega}} = \mathbf{0}$, then we have $-\boldsymbol{f}(\mathbf{0}, \boldsymbol{P}) = \boldsymbol{G}(\boldsymbol{P}, \boldsymbol{\delta})$. The desired moment vector will then be defined as $\boldsymbol{d}_{des} = -\boldsymbol{f}(\mathbf{0}, \boldsymbol{P})$. Thus, we have

$$\boldsymbol{d}_{des} = -\begin{bmatrix} \bar{L}_{base}(M,\alpha) \\ M_{base}(M,\alpha) \\ N_{base}(M,\alpha) \end{bmatrix} = \begin{bmatrix} 0 \\ -M_{base}(M,\alpha) \\ 0 \end{bmatrix} \tag{74}$$

where $\bar{L}_{base}$ is the wing-body rolling moment, M_{base} is the wing-body pitching moment, and N_{base} is the wing-body yawing moment. Typically symmetric flight (i.e., zero sideslip angle) is assumed; therefore, the side force and $\bar{L}_{base}$ and N_{base} are taken to be zero. Note the presence of the minus sign above in Equation 74. The minus sign is present because we want to counteract the wing-body moment with the control effectors to achieve rotational equilibrium; therefore, we desire the moment produced by the effectors to be of opposite sign to that of the base moments. More details on the algorithm can be found in Reference [11].

Shown in Figure 5 is an example of the moment deficiency for the X-33 vehicle model used by Shaffer [12]. The X-33 has a suite of 8 effectors: right and left body flaps, right and left rudders, and right and left inboard and outboard elevons. In Figure 5 the contours of the trim deficiency as a function of Mach and α are given. The failure that is considered is a double body-flap stuck at 26 deg trailing edge down. A non-zero value of the control deficiency, $\|\boldsymbol{d}_{des} - \boldsymbol{G}(\boldsymbol{\delta})\|_2$, indicates that vehicle cannot be trimmed at that particular Mach number and angle-of-attack. Notice that the region over which the aircraft can be trimmed is significantly reduced. Only below bout Mach 0.25 can the vehicle be trimmed at any angle-of-attack. Figures 6 and 7 demonstrate the change in lift and drag over the flight envelope. Note that a negative ΔC_D indicates an increase in drag and a negative ΔC_L indicates an increase in lift compared to the un-failed case.

Of particular importance when computing the trim map

Algorithm 1 Trim Map Generation

Define a grid for Mach number and angle-of-attack and discretize such that $M = \{M_1, \ldots, M_i, \ldots, M_M\}$ and $\alpha = \{\alpha_1, \ldots \alpha_j, \ldots, \alpha_N\}$
for $i = 1$ to M **do**
  for $j = 1$ to N **do**
    Determine the wing-body moments, $\boldsymbol{d}_{des} = \begin{bmatrix} 0 \\ -M_{base}(M_i, \alpha_j) \\ 0 \end{bmatrix}$
    Pick the preference vector, $\boldsymbol{\delta}_p$
    Solve the control allocation problem for $\boldsymbol{\delta}$ given $\boldsymbol{d}_{des}$ and $\boldsymbol{\delta}_p$
    Compute the control deficiency

$$\Delta_{i,j} = \|\boldsymbol{d}_{des} - \boldsymbol{G}(\boldsymbol{\delta}, \boldsymbol{P})\|_2$$

    Compute the lift and drag at (M_i, α_j) using $\boldsymbol{\delta}$ obtained above.
  end for
end for

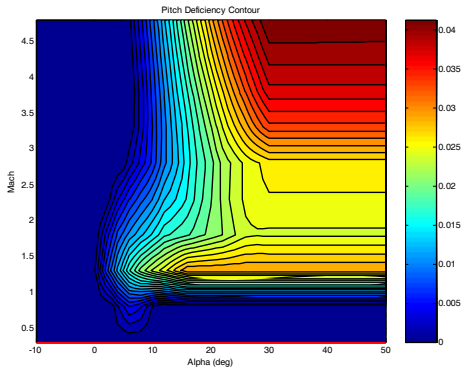

Fig. 5. Moment Deficiency for a 26 deg Body Flap Failure

is the selection of the preference vector, $\boldsymbol{\delta}_p$. The moment deficiency is independent of the preference vector since it is determined solely by the control deficiency branch of the cost function: $\|\boldsymbol{d}_{des} - \boldsymbol{G}(\boldsymbol{\delta}, \boldsymbol{P})\|_1$. At the trimmable Mach-$\alpha$ points, there may exist non-unique solutions to the control allocation problem, thus the trim effects on the lift and drag are effected by the deflection of the remaining effectors. Computing the lift and drag effects allows us to capture 6 degree-of-freedom effects in the reduced order models used for trajectory synthesis. Figures 8 and 9 show the effects of the preference vector on the lift and drag coefficients for the nominal, unfailed case. The two preference vectors being compared are a minimum drag preference vector, $\boldsymbol{u}_{pref} = \mathbf{0}$, and a maximum drag case where $\boldsymbol{u}_{pref}$ was set at the upper limit for all effectors. Figures 8 and 9 indicate the level of sensitivity of the lift and drag coefficient to the preference vector.

The objective that one is trying to obtain when performing trajectory synthesis must be kept in mind when selecting the

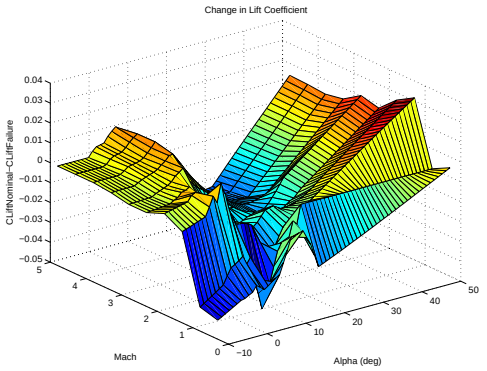

Fig. 6. Lift Coefficient Perturbation Due to Body Flaps Failed at 26 deg

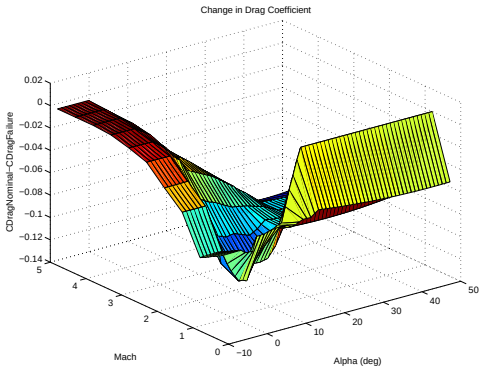

Fig. 7. Drag Coefficient Perturbation Due to Body Flaps Failed at 26 deg

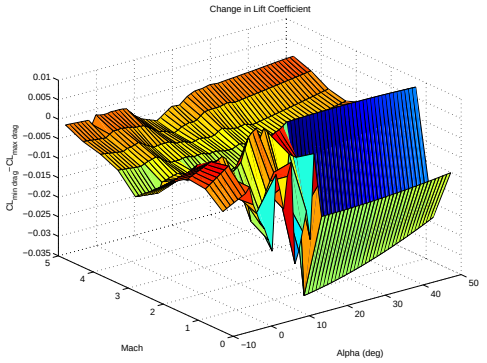

Fig. 8. Change in Lift Coefficient Due to Preference Vector for No Failures

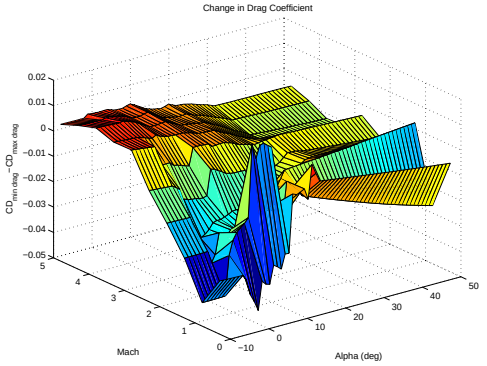

Fig. 9. Change in Drag Coefficient Due to Preference Vector for No Failures

preference vector. An obvious situation where an inappropriate choice of the control preference vector in the control allocation can have a negative implication is when determining the landing footprint [12]. For example, selecting a preference vector to minimize the drag on the vehicle when trying to compute the *minimum* downrange will produce an erroneous solution. In order to minimize downrange, it is desired to minimize total L/D for the vehicle. Therefore, the control allocator should be set to meet the moment demand while increasing the trim drag and decreasing the trim lift. Conversely, to maximize the downrange, one wants to maximize L/D. Therefore, to minimize the trim drag, the preference vector should be set to $\boldsymbol{\delta}_p = \mathbf{0}$. Poor selection of the preference vector will result in the control allocation having unintended, adverse effects on the trajectory.

V. Conclusions

A method was presented for the solution of a class of non-linear control allocation problems. Control allocation has historically been performed by assuming that a linear relationship exists between the control induced moments and the control effector displacements. Since aerodynamic data almost always exhibits non-linear behavior, such assumptions can lead to degraded performance or vehicle loss when secondary non-linear effects must be used to control a vehicle, particularly after control effector failures have occurred. Aerodynamic databases are usually discrete-valued and are almost always stored in multi-dimensional look-up tables where it is assumed that the data is connected by piecewise linear functions.

The approach that was presented assumes that the control effector moment data is piecewise linear. This assumption allows us to cast the control allocation problem as a piecewise linear program. In order to solve the piecewise linear program, it was re-formulated as a mixed-integer linear program and solved using a readily available branch-and-bound algorithm. Simulation showed that the piecewise linear programming formulation results in improved tracking performance of the desired moments when compared to a more traditional control allocation approach that uses the linear assumption, especially when the aircraft is forced to operate with its control effectors in non-linear portions of the control moment curves as a result of control effector failures. The piecewise linear control allocator was able to maintain control of the aircraft and land after the failures were introduced while a control allocation algorithm that utilized a simple linear relationship along with an intercept correction term did not. The piecewise linear control allocator was applied to the determination of regions of trimmable angle-of-attack and Mach number for the purposes of trajectory reshaping under failure conditions. We also discussed the effects of the choice of preference vector to estimate trim lift and trim drag in conjunction with the reduced order trajectory optimization algorithms.

References

[1] D. Enns, "Control allocation approaches," in *Proceedings of the 1998 AIAA Guidance, Navigation, and Control Conference*, pp. 98–108, AIAA Paper No. AIAA1998-4109.

[2] J. Buffington, "Modular Control Law Design for the Innovative Control Effectors (ICE) Tailless Fighter Aircraft Configuration 101-3," Air Force Research Laboratory, Wright-Patterson AFB, OH, Tech. Rep. AFRL-VA-WP-TR 1999-3057, June 1999.

[3] M. Bodson, "Evaluation of Optimization Methods for Control Allocation," *Journal of Guidance, Control, and Dynamics*, vol. 25, no. 4, pp. 703–711, 2002.

[4] W. Durham, "Constrained Control Allocation: Three-Moment Problem," *Journal of Guidance, Control, and Dynamics*, vol. 17, no. 2, pp. 330–336, 1994.

[5] D. Doman and M. Oppenheimer, "Improving Control Allocation Accuaracy for Nonlinear Aircraft Dynamics," in *Proceedings of the AIAA Guidance, Navigation, and Control Conference*, May 2002, AIAA Paper No. AIAA2002-4667.

[6] M. A. Bolender and D. B. Doman, "Non-linear Control Allocation Using Piecewise Linear Functions," *Journal of Guidance, Control, and Dynamics*, vol. 27, no. 6, pp. 1017–1027, Nov./Dec. 2004.

[7] G. Reklaitis, A. Ravindran, and K. Ragsdell, *Engineering Optimization: Methods and Application*. New York: Wiley-Interscience, 1983, pp. 314-324.

[8] D. Bertsimas and J. Tsitsiklis, *Introduction to Linear Optimization*. Belmont, MA: Athena Scientific, 1997, pp. 15-18, pp. 455-456.

[9] J. Schierman, J. Hull, and D. Ward, "On-line Trajectory Command Reshaping for Reusable Launch Vehicles," in *Proceedings of the 2003 AIAA Guidance, Navigation, and Control Conference [CD-ROM]*, August 2003, AIAA Paper No. 2003-5439.

[10] P. Chandler, M. Pachter, and M. Mears, "System Identification for Adaptive and Re-configurable Control," *Journal of Guidance, Control, and Dynamics*, vol. 18, no. 3, pp. 516–524, 1995.

[11] F. Fahroo and D. Doman, "A direct method for approach and landing trajectory reshaping with failure effect estimation," AIAA Paper No. AIAA2004-4772.

[12] P. Shaffer, "Optimal Trajectory Reconfiguration and Re-targeting for the X-33 Reusable Launch Vehicle," Master's thesis, Naval Postgraduate School, Monterey, CA, Sept. 2004.